



Nonlinear absorption of light: two-photon absorption and optical saturation in metalloporphyrin-doped boric acid glass

T.C. Wen^{*}, L.C. Hwang, W.Y. Lin, C.H. Chen, C.H. Wu

Department of Chemistry, Kaohsiung Medical University, P.O. Box 72-94, Kaohsiung, Taiwan, ROC

Received 4 June 2002

Abstract

The nonlinear absorption of five metal TMPPs (TMPP: tetrakis-(3,4,5-trimethoxyphenyl)porphyrin) doped in boric acid glass are measured with the linear polarized nanosecond laser pulses at different wavelengths by Z-scan; the two-photon absorption (TPA) is dominant in the near infrared, while the characteristic of saturation absorption (SA) is observed close to the Q(0,0) band of porphyrin. The symmetry allowed two-photon $\pi^* \leftarrow \pi$ transitions are suggested to be ${}^1B_{1g}^* \leftarrow S_0$ and ${}^1B_{2g}^* \leftarrow S_0$, with the cross-sections δ ranging from 25×10^{-50} to 114×10^{-50} cm⁴ s/photon. We analyze the property of SA with a four-level system, and find that the magnitudes of excited-state absorptivity and saturation intensity are not affected by changing the central metal ion in these experiments.

© 2002 Elsevier Science B.V. All rights reserved.

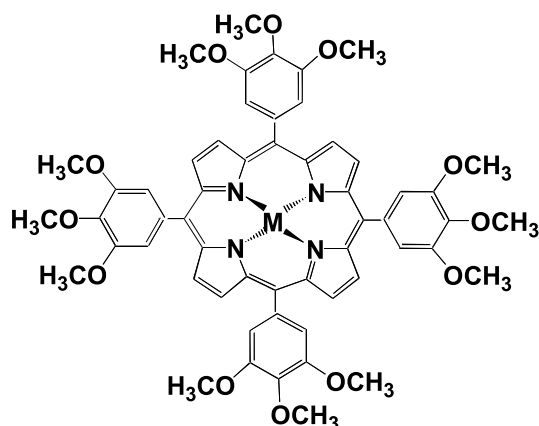
1. Introduction

For the porphyrin derivatives such as tetrabenzoporphyrin (TBP) and tetraphenylporphyrin (TPP), large third-order nonlinear susceptibility $\chi^{(3)}$ and cross-sections of the excited-state absorption (RSA) have been recognized with both nanosecond and picosecond laser pulses at 532 nm [1–4]. More recently, the RSA in TPP complexes including a variety of central metal ions (e.g. Cd(II), Sn(II), Pb(II) and P(V)Cl₂) are measured with the Z-scan technique at 532 nm; enhancement of RSA by the heavy-atom effect is revealed [5–8].

Meanwhile, the nonlinear transmission of metal free porphyrin (H₂TPP) derivatives are studied at different wavelengths; for example, in a solid matrix environment (doped in boric acid glass), they display saturation absorption at the argon-ion laser wavelengths of 458 and 476.5 nm [9], whereas in toluene solutions, no transmittance variations are observed using 784 nm (60 fs) pulses from a self-mode-locked Ti:sapphire laser [10]. The present paper is devoted to the investigation of nonlinear absorption of metal TMPP (TMPP: tetrakis-(3,4,5-trimethoxyphenyl)porphyrin) including chlorogallium(III), chloroindium(III), chlorothallium(III), tin(II) and lead(III) as central metal ions. These materials are doped in a solid matrix (boric acid) and measured with nanosecond laser pulses from 650 to 1350 nm (see Fig. 1).

^{*} Corresponding author. Tel.: +886-7-312-1101; fax: +7-312-5339.

E-mail address: tschwe@cc.kmu.edu.tw (T.C. Wen).



M = Group IIIa: GaCl(III), InCl(III), TlCl(III),
Group IVa: Sn(II), Pb(II),

Fig. 1. Molecular structures of metal TMPPs.

2. Experimental

The free base H_2TMPP is prepared from pyrrole and 3,4,5-trimethoxybenzaldehyde by the method of Chan et al. [11] Chromatographic purification is repeated on silica gel columns and the final products are identified by NMR and elemental analysis. The metal TMPP is prepared by refluxing H_2TMPP and one of the metal halides (e.g. $GaCl_3$ and $InCl_3$) or metal acetate (e.g. $(CH_3CO_2)_2Pb \cdot 3H_2O$) in benzonitrile or dimethylformamide [12], and the crystallized products are identified by NMR and UV-Vis spectroscopy. The preparation of metal TMPP-doped boric acid glass that we adopted is different from that used previously [13,14]. Appropriate quantities of porphyrin and boric acid are measured and mixed thoroughly and a suitable amount of this mixture is spread uniformly over the microscopic glass slide. Another microscope slide is used to make a sandwich of the sample. This sample is then heated in a high temperature oven at 190 ± 2 °C for an hour. After that, the temperature is raised to 200 ± 2 °C and the sample is heated for one more hour. The samples obtained are of good linear transmittance (~ 70 – 90%), and most of the porphyrin molecules are not decomposed according to their UV-Vis absorption spectra. Sample thickness is in the

range ~ 50 – 100 μm as measured with a micrometer, and the concentration of the porphyrin molecules is $\sim 10^{-2}$ M (i.e. $\sim 8.0 \times 10^{18}$ number of molecules/ cm^3).

The UV-Vis absorption spectra are measured with a Shimadzu UV-160A spectrophotometer, while the oscillator strength f is evaluated from the data by the formula $f = 4.33 \times 10^{-9} \epsilon \Delta\nu$, where ϵ is the maximum molar extinction coefficient in $(cm \text{ mol/L})^{-1}$ and $\Delta\nu$ is the band width at half-maximum in cm^{-1} .

The nonlinear optical responses are performed from 650 to 1350 nm. These laser pulses are generated by an optical parametric oscillator (OPO) (Continuum Surelite) pumped by the third harmonic of a Nd:YAG laser. The beam from the OPO laser (with 5 ns pulse width) is expanded to 20 mm in diameter and subsequently passed through a 3.0 mm-diam aperture, which gives the beam a nearly flat top intensity profile [15,16]. To turn the linear-polarized light from OPO (which is horizontally polarized) into circularly polarized light, a $\lambda/4$ zero-order waveplate (from CVI Laser Corporation) is inserted between the source and the Glan-laser calcite polarizer ranging from 1000 to 1550 (from Newport) which is also horizontally polarized as the input light. The waveplate is rotated around the beam axis to find the orientation that retains the extinction, then rotate this plate 45° from this position to obtain half the input light passing through the Glan-laser polarizer. The quality of the circularly polarized light is also adjusted by tilting the waveplate about its fast (or slow) axis.

For an open aperture Z-scan, a focal lens (76 mm in diameter) is mounted 15 cm just behind the focal point of the incident laser pulses ($\omega_0 \approx 20$ μm) which is focused with a lens of 10 cm focal length. The incident and transmitted energies are detected simultaneously by two energy probes Rjp-735 (pyroelectric based) and Rjp-765 (silicon based), then averaged with RJ-7620 (Laser Precision) energy meter individually. Each data point is an average of over 50 shots with 0.5 Hz repetition rate. The experimental errors are estimated to be $\pm 15\%$ from the variations of laser energies and sample concentrations.

3. Results and discussion

The absorption spectra of all metal TMPPs doped in boric acid are shown in Fig. 2(a), and the absorption spectra of these compounds in CH_2Cl_2 solutions are also plotted in Fig. 2(b) for comparison. Due to the interaction between the p_π (or d_π) metal orbital and the ring a_{2u} (or e_g) orbital, the intensity of the Q(0,0) absorption band is sensitive to variations of the coordinated central metal ion and ligand [17]. For the metal TMPP in solution, its oscillator strength of Q(0,0) band is enhanced by the metal ion following the order of $\text{GaCl(III)} < \text{InCl(III)} < \text{TlCl(III)}, \text{Sn(II)} < \text{Pb(II)}$, while the λ_{max} of Q(0,0) band shifts to the red with the same

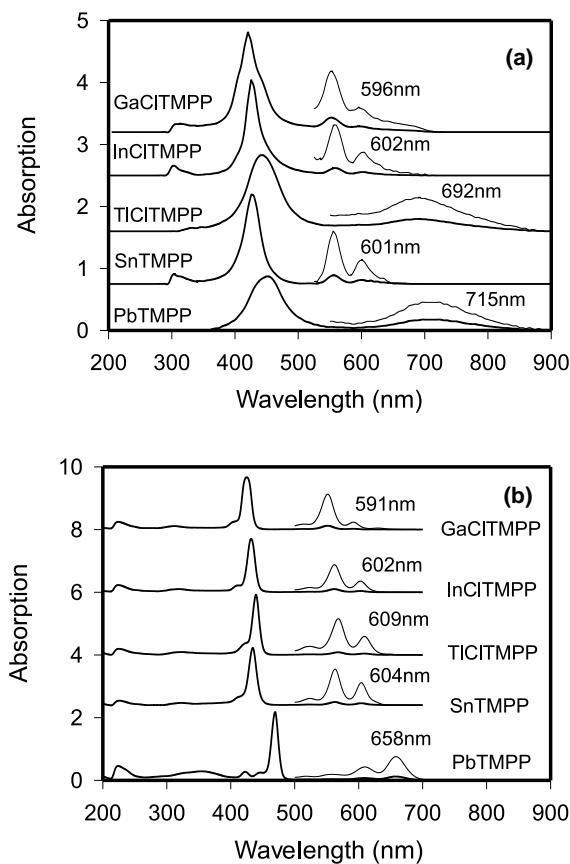


Fig. 2. The ground state absorption bands B(0,0), Q(1,0) and Q(0,0) of metal TMPP (a) doped in boric acid, and (b) in CH_2Cl_2 solutions. λ_{max} of Q(0,0) band is indicated in each of them.

order, Table 1. Similar results are observed for metal TMPP-doped in boric acid except TICITMPP and PbTMPP: their Q(0,0) and Q(1,0) bands (usually appear in liquid solution) are replaced with much broader bands peaked at 692 and 715 nm, respectively. This property could be induced by the acidic environment of the boric acid [18]. For example, protonation by trifluoroacetic acid of a free-based TPP in CH_2Cl_2 gives rise to new types of spectra: the spectrum of the centrally protonated porphyrin shows a broad and flat absorption in the visible (with $\lambda_{\text{max}} \approx 654$ nm) for its Q-bands [19]. This behavior is interpreted as a “hyperporphyrin spectra” in terms of charge-transfer excited states which involve charge movement either into or out of the porphyrin ring [19].

3.1. The nonlinear absorptions dominated by the TPA

The open aperture Z-scan traces of the sample at four different wavelengths are recorded. The excitation energy is approximately $10 \mu\text{J}$ ($\sim 13.2 \times 10^7 \text{ W/cm}^2$ at the focus). As displayed in Fig. 3, all the transmission curves are symmetric with respect to the focus ($z = 0$), where they exhibit a nonlinear absorption that we suggested to be caused by the TPA.

The molecular orbital ordering and the one- and two-photon properties of porphyrins have been investigated theoretically [17,20–22]. A semi-empirical SCF-MO calculation indicates that, for a free base porphyrin dianion molecule belonging to the D_{4h} point group, its lowest-lying two-photon allowed states belong to the ${}^1B_{1g}^*$ and ${}^1B_{2g}^*$ irreducible representations [20]. The calculated $\pi^* \leftarrow \pi$ transition energy, ΔE (eV), is 3.17 eV (${}^1B_{1g}^* \leftarrow S_0$) and 3.52 eV (${}^1B_{2g}^* \leftarrow S_0$), which are lying in the Soret (B-band) region. However, these states are highly sensitive to environment; [20] for example, the ${}^1B_{1g}^*$ state of a D_{2h} free base porphyrin moves from 3.134 to 2.53 eV as the external electric field intensities increase from 1×10^6 to $5 \times 10^7 \text{ V/cm}$. As emphasized in [20], such field intensities are experienced by porphyrins embedded in proteins, as typical polar group-to-chromophore distances of $< 5 \text{ \AA}$ can generate field intensities greater than $5 \times 10^7 \text{ V/cm}$. Besides, the focused laser radiation

Table 1
UV-Vis spectroscopic parameters of (a) metal TMPP doped in boric acid glass, and (b) in CH₂Cl₂ solutions

Compound of metal TMPP	Molecular weight of metal TMPP (g/mol)	Concentration of metal TMPP in boric acid	λ_{max} and energy (eV) of B(0,0)	λ_{max} and energy (eV) of Q(1,0)	λ_{max} and energy (eV) of Q(0,0)	$f_{Q(0,0)}$ ($\times 10^{-3}$)
GaCITMPP	1103.2	1.3×10^{-2} mol/L or 7.83×10^{18} no. of molecules/cm ³	421 nm (425 nm) 2.95 eV	553 nm (552 nm) 2.24 eV	596 nm (591 nm) 2.08 eV	(14.09)
InCITMPP	1148.3	1.28×10^{-2} mol/L or 7.74×10^{18} no. of molecules/cm ³	426 nm (431.4 nm) 2.91 eV	556 nm (561 nm) 2.23 eV	602 nm (602 nm) 2.06 eV	(30.33)
TiCITMPP	1237.9	1.18×10^{-2} mol/L or 7.10×10^{18} no. of molecules/cm ³	443 nm (439.4 nm) 2.80 eV	(567.5 nm)	692 nm* (609 nm) 1.79 eV	(46.45)
SnTMPP	1116.7	1.34×10^{-2} mol/L or 8.05×10^{18} no. of molecules/cm ³	427 nm (436.2 nm) 2.90 eV	556 nm (563.0 nm) 2.23 eV	601 nm (604 nm) 2.06 eV	(66.52)
PbTMPP	1205.2	1.20×10^{-2} mol/L or 7.19×10^{18} no. of molecules/cm ³	450 nm (469.2 nm) 2.75 eV	(609.5 nm)	715 nm* (658 nm) 1.73 eV	(135.66)

Data in parentheses are measured from CH₂Cl₂ solutions, where $f_{Q(0,0)}$ is the oscillator strength of Q(0,0) band determined in CH₂Cl₂.
* TCITMPP and PbTMPP doped in boric acid glass have a broad band with λ_{max} equals 692 and 715 nm, respectively.

used in two-photon studies will typically produce transient electric fields in the range 10^4 – 10^5 V/cm and field intensities from 10^6 to $>10^7$ V/cm are possible [21]. On the other hand, the all valence electron SCF-MO calculations indicate that, among those porphyrins and metal porphyrins that possess D_{4h}, D_{2h} or C_{4v} symmetry point groups, the energies of their highest filled a_{1u}(π) and a_{2u}(π) states are almost the same [22].

The TPA in metal TMPPs, therefore, is suggested tentatively to initiate from the S₀ (i.e. ¹A_{1g}) state, and attend one of the final states following the processes of ¹B_{1g}* ← S₀ (for 840 and 900 nm laser light) and ¹B_{2g}* ← S₀ (for 1200 and 1350 nm light), as illustrated in Fig. 4(a).

During the TPA, the rate equation of light propagation in the sample is

$$\frac{dI}{dz} = -(\alpha_0 + \beta I)I, \quad (1)$$

where α_0 is the linear absorption coefficient ($\alpha_0 = (\ln(1/T))/L$), and β is the two-photon absorption coefficient. The values of α_0 and β can be assumed as constants at certain light intensities, thus Eq. (1) is integrated to give

$$\int_{I_{\text{in}}}^{I_{\text{out}}} \frac{1}{I} dI - \int_{I_{\text{in}}}^{I_{\text{out}}} \frac{1}{I + (\alpha/\beta)} dI = -\alpha_0 L, \quad (2)$$

where I_{in} and I_{out} are the input and output intensities, respectively. The solution gives

$$I_{\text{out}}(z, r, t) = I_{\text{in}}(z, r, t) e^{-\alpha_0 L} \left/ \left\{ 1 + \frac{I_{\text{in}}(z, r, t) \beta (1 - e^{-\alpha_0 L})}{\alpha_0} \right\} \right. \quad (3)$$

The normalized transmittance for the open aperture Z-scan is then obtained by integrating of Eq. (3) over the spatial extent of the laser beam [23]

$$T(z) = 1 - \frac{q_0}{2\sqrt{2}} \quad \text{for } |q_0| < 1, \quad (4)$$

where

$$q_0(z, t) = \beta I_0 L_{\text{eff}} \frac{1}{1 + z^2/z_0^2}, \quad (5)$$

I_0 is the on-axis instantaneous intensity at focus ($z=0$) and L_{eff} is the effective sample thickness given by $L_{\text{eff}} = (1 - \exp[-\alpha_0 L])/\alpha_0$.

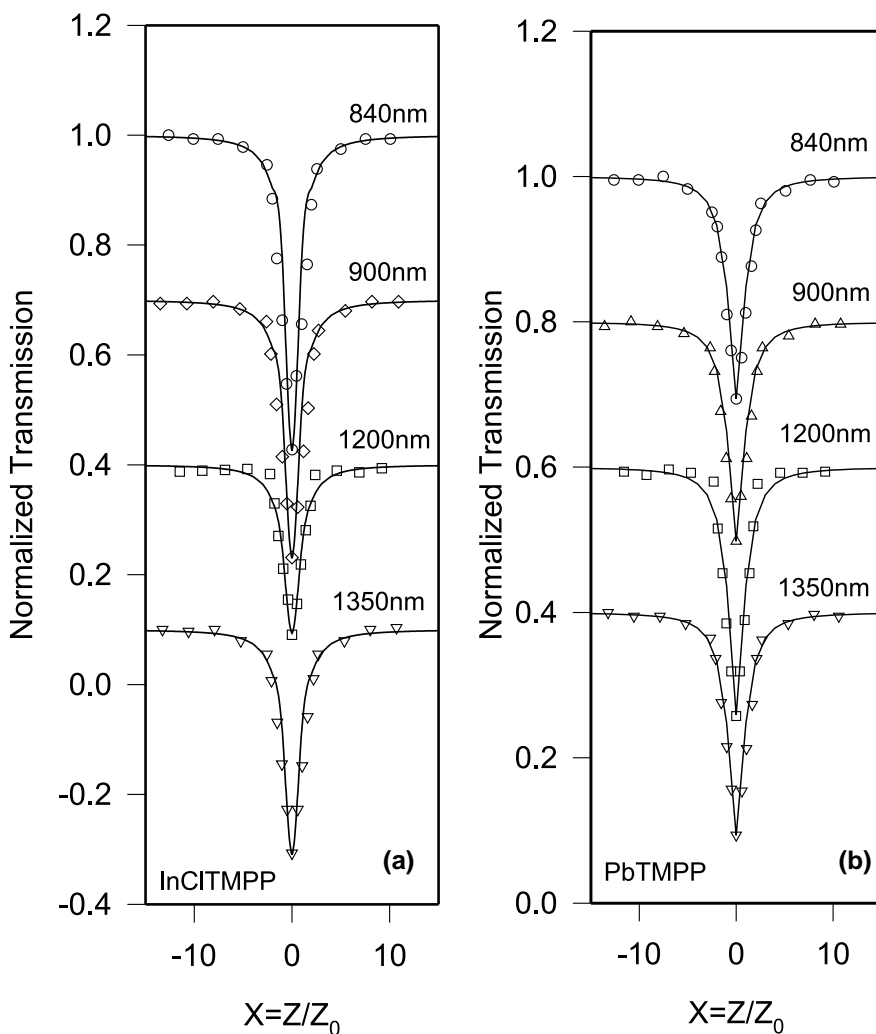


Fig. 3. Normalized transmittances from boric acid glasses doping with (a) InCITMPP and (b) PbTMPP. The curves are moved from their original positions for the clear vision. The solid curves are the fit with Eq. (4).

The TPA coefficient β (in units of cm/GW) is therefore deduced from the best fitting of our Z-scan data with Eqs. (4) and (5), and the TPA cross-section δ (in units of cm⁴ s/photon) is evaluated by using the following relationship:

$$\delta = \frac{hv\beta}{N_A d_0 \cdot 10^{-3}}, \quad (6)$$

where hv is the energy of an incident photon, d_0 is the concentration of the dopant compound in boric acid (in units of M/L), and finally N_A the Avogadro number. As listed in Table 2, the mea-

sured δ are ranging from 25×10^{-50} to 54×10^{-50} cm⁴ s/ photon (for the process of ${}^1B_{1g}^* \leftarrow S_0$), and from 31×10^{-50} to 114×10^{-50} cm⁴ s/photon (for the process of ${}^1B_{2g}^* \leftarrow S_0$). As we mentioned before, the near infrared light from our OPO laser is linear polarized with horizontal polarization (i.e. the transmission axis is parallel to the surface of our laser table). Under the same arrangements, we predict that δ in a free base porphyrin dianion are around 20.8×10^{-50} cm⁴ s/photon (for ${}^1B_{1g}^* \leftarrow S_0$) and 1.7×10^{-50} cm⁴ s/photon (for ${}^1B_{2g}^* \leftarrow S_0$) [20].

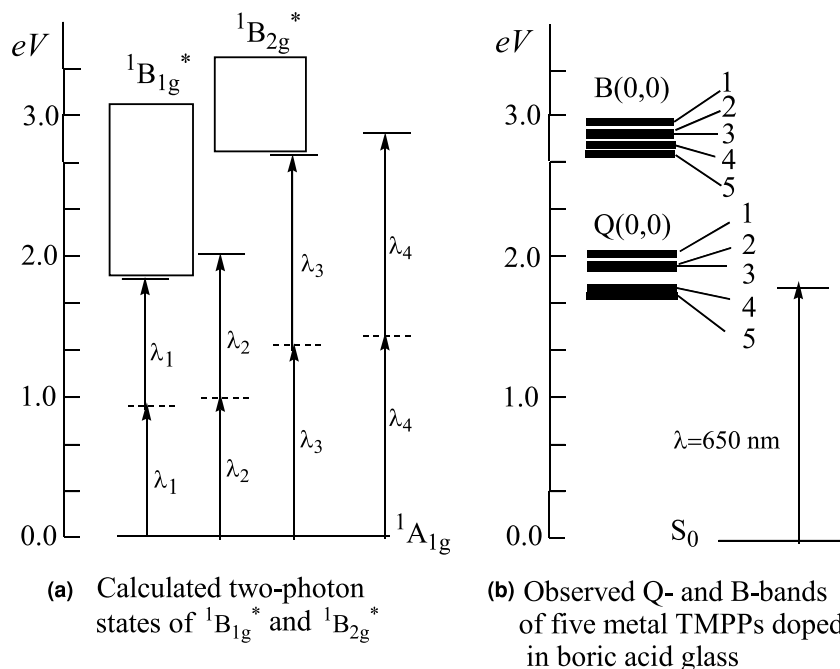


Fig. 4. Schematic representation of (a) the theoretical calculated two-photon states of a D_{4h} free base porphyrin dianion [20]. Transitions proceeded by the laser beams of λ_1 (1350 nm), λ_2 (1200 nm), λ_3 (900 nm) and λ_4 (840 nm) are also illustrated. In (b), the observed B(0,0)- and Q(0,0)-band energies of porphyrin derivatives are plotted according to 1. GaCITMPP, 2. InCITMPP, 3. SnTMPP, 4. TICITMPP and 5. PbTMPP.

In addition, the characteristics of two-photon excited states can be verified from the polarization ratio $\Omega = \langle \delta_{\text{circ}} \rangle / \langle \delta_{\text{lin}} \rangle$, where $\langle \delta_{\text{circ}} \rangle$ and $\langle \delta_{\text{lin}} \rangle$ are the two photon absorptivities under circular and linear polarization, respectively. For ${}^1B_{1g}^*$ and ${}^1B_{2g}^*$ (D_{4h}) states, in the absence of vibronic coupling

$$\Omega = \frac{3(S_{\alpha\beta}S_{\alpha\beta}^* + S_{\alpha\beta}S_{\beta\alpha}^*)}{2(S_{\alpha\beta}S_{\alpha\beta}^* + S_{\alpha\beta}S_{\beta\alpha}^*)} = \frac{3}{2}, \quad (7)$$

where $(S_{\alpha\beta}S_{\alpha\beta}^*)$ is a product of two second-rank tensors which are functions of the internal molecular Cartesian coordinates α and β and the photon and state energies [20]. Using the Z-scan method, we measure the absorptivities of InCITMPP and GaCITMPP (doped in boric acid) with both circular and linear polarized light at 1320 nm. The results give $\Omega = 1.40$ ($\Omega = \delta_{\text{circ}}/\delta_{\text{lin}} = \beta_{\text{circ}}/\beta_{\text{lin}} = (0.21 \text{ cm/GW})/(0.15 \text{ cm/GW})$) for InCITMPP (see Fig. 5) and $\Omega = 1.43$ ($\Omega = (0.20 \text{ cm/GW})/(0.14 \text{ cm/GW})$) for GaCITMPP. To con-

firm these two-photon excited states, we are arranged to determine this polarization ratio at some specific wavelengths (e.g. 840 and 1200 nm) in the near future.

The behavior of TPA in the near infrared (1350 nm) is also observed from the incident intensity-dependent experiments (see Fig. 6); we measure the transmitted intensity I passing through a sample by various input intensities I_0 , and fit the data with a formula

$$I = \frac{I_0}{(1 + I_0\beta L)}, \quad (8)$$

where L is the thickness of the sample. Eq. (8) is derived from the rate equation of light propagation (that is Eq. (1)) with the assumptions that $\alpha_0 \approx 0$ (transparent sample) and the beam has a nearly uniform transverse intensity distribution within the sample [24]. As listed in Table 2, β obtained here is in good agreement with its Z-scan result.

Table 2
Two-photon absorption coefficient β and cross-section δ in metal TMPP doped in boric acid glass

Compound	Excitation wavelength (nm)	TPA coefficient β (cm/GW)	TPA cross-section δ ($\times 10^{-50}$ (cm ⁴ s/photon))	Imaginary part of third-order $\chi^{(3)}\text{Im}\chi^{(3)}$ ($\times 10^{-12}$ esu)
GaCITMPP	840	0.11	31	0.67
	900	0.13	36	0.85
	1200	0.27	54	2.37
	1350	0.14 (0.12)	25 (22)	1.39
InCITMPP	840	0.38	114	2.38
	900	0.22	65	1.45
	1200	0.22	47	1.92
	1350	0.19 (0.22)	36 (39)	1.91
TICITMPP	840	0.19	52	1.17
	900	0.21	57	1.42
	1200	0.13	26	1.15
	1350	0.18 (0.21)	32 (36)	1.81
SnTMPP	840	0.22	64	1.35
	900	0.11	31	0.63
	1200	0.38	77	3.43
	1350	0.18 (0.22)	32 (39)	1.80
PbTMPP	840	0.19	56	1.19
	900	0.16	43	1.12
	1200	0.34	67	2.98
	1350	0.18 (0.21)	32 (36)	1.70

Data in parenthesis are determined by the intensity-dependent transmittance method. All the excitation pulses are linear polarized with horizontal polarization.

In cgs units, the imaginary part of the third-order nonlinear susceptibility $\chi^{(3)}$ is related to the TPA coefficient β through

$$\text{Im}\chi^{(3)} = \frac{n_0^2 \epsilon_0 \lambda C}{2\pi} \beta, \quad (9)$$

where n_0 is the linear index of refraction ($n_0 = 1.37$ for boric acid glass), ϵ_0 is the permittivity of

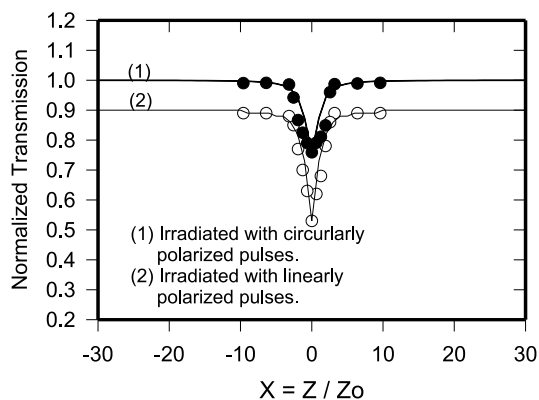


Fig. 5. Normalized transmittances from InCITMPP doped in boric acid (~ 0.01 M). The input intensity is around $6 \mu\text{J}$ at 1320 nm. Curve (1) is irradiated with circularly polarized pulses and curve (2) is irradiated with linearly polarized pulses, while curve (2) is moved downward from original position for the clear vision. Both solid curves are the fit with Eq. (4).

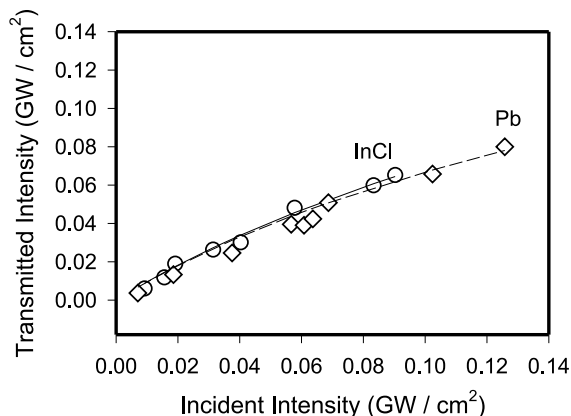


Fig. 6. Measured transmitted intensity as a function of the incident intensity (at 1350 nm) for InCITMPP (open cycle) and PbTMPP (open diamond). The solid curves are fitted with Eq. (7).

vacuum ($\epsilon_0 = (1/4\pi) \text{esu}^2/\text{erg}/\text{cm}$), λ is the wavelength of incident light and C is the speed of light in vacuum. Thus $\text{Im}\chi^{(3)} \propto 0.63 \times 10^{-12} - 3.43 \times 10^{-12} \text{esu}$ from the calculations.

3.2. The nonlinear absorptions dominated by the SA

When an organic dye (e.g. fluorescein-doped boric acid glass) is irradiated by a strong laser pulse, the large $S_0 \rightarrow S_1$ absorptivity ($\approx 10^{-16} \text{cm}^2$) always leads to a substantial transient population in the S_1 state; meanwhile, the population builds up in the lowest excited triplet state (T_1) via intersystem crossing. In addition, because many of the quenching mechanisms that are present in liquid do not exist in a solid matrix, the lifetime of T_1 state is very long in a solid environment; for examples, in fluorescein-doped boric acid glass, the decay of its triplet state population is $\geq 100 \text{ms}$, [13] while the measured triplet lifetimes in porphyrin-doped boric acid glass is about $200 \mu\text{s}$ [9]. Thus, a four-level system (in Fig. 7) seems adequate to describe the saturation absorption in solid porphyrin samples [13,25]. For the sake of simplicity, we assume that (1) the $3 \rightarrow 2$ and $4 \rightarrow 2$ transitions are fast (compared with the excitation pulse duration), and (2) all of the initially excited molecules ($1 \rightarrow 3$) are trapped in level 2 (T_1), which is the only state leading to excited-state

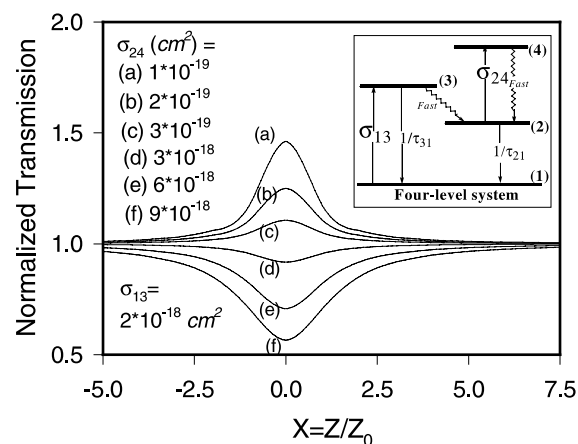


Fig. 7. A four-level system (inset picture) together with the change of transmitted light vs. different excited-state absorption cross-sections as described in Section 3.2.

absorption. The change in intensity of the light as it passing through this model is therefore governed by $dI/dz = -\alpha(I)I$, where $\alpha(I) = \alpha_0 + \beta_0$; α_0 is the linear and β_0 is the nonlinear absorption coefficients arising from the transitions of $1 \rightarrow 3$ and $2 \rightarrow 4$, respectively. Furthermore, the value of β_0 is proportional to the number of molecules, $N(t)$, in T_1 state: $\beta_0 = \sigma_{24}N(t)$. Thus the equations governing the absorption can be expressed as:

$$\frac{dI}{dz} = -(\alpha_0 + \sigma_{24}N(t))I, \quad (10)$$

$$\frac{dN(t)}{dt} = \frac{\alpha_0 I}{\hbar\omega}, \quad (11)$$

where $\hbar\omega$ is the energy of the laser pulse. Eqs. (8) and (9) can be combined to yield

$$\frac{dI}{dz} = -\alpha_0 I - \frac{\sigma_{24}\alpha_0 I}{\hbar\omega} \int_{-\infty}^t I(t') dt'. \quad (12)$$

This equation is solved for the fluence and integrated over the spatial extent of the laser beam to yield the normalized transmission T , given by [2]

$$T = \ln \left(1 + \frac{q_0}{1+x^2} \right) / \frac{q_0}{1+x^2}, \quad q_0 = \frac{\sigma_{24}\alpha_0 F_0 L_{\text{eff}}}{2\hbar\omega}, \quad (13)$$

where $x = z/z_0$, z is the position of the sample and z_0 is the Rayleigh range of the lens and F_0 is the fluence (J/cm^2) of the laser at focus ($z = 0$).

Thus the behavior of saturation absorption can be simulated with Eq. (13): let $\sigma_{13} = 2 \times 10^{-18} \text{cm}^2$, $F_0 = 1.733 \text{J}/\text{cm}^2$ (corresponding to $E = 17 \mu\text{J}$) and $\hbar\omega = 3.06 \times 10^{-19} \text{J}$ (at 650nm) in this equation. With the cross-section σ_{24} decreases from 3×10^{-19} to $1 \times 10^{-19} \text{cm}^2$, we obtain a normalized transmittance that increases from ~ 1.15 to ~ 1.50 as a result. On the other hand, when the size of σ_{24} is larger than that of the ground state σ_{13} , the characteristic of reverse saturable absorption (RSA) is presented as plotted in Fig. 7.

The normalized transmittances from metal TMPPs at 650nm are shown in Fig. 8, where each of them has a maximum transmittance at the focal point. The solid curves through the experimental data represent the theoretical fits with Eq. (13); we obtain σ_{24} ranging from 3.36 to $3.91 \times 10^{-19} \text{cm}^2$.

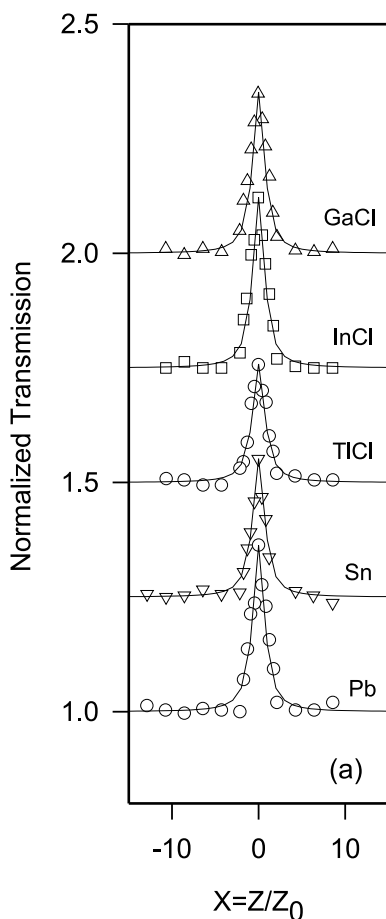


Fig. 8. The saturation absorption at 650 nm of five metal TMPP samples. The solid curves are the fittings of data to Eq. (13).

The ground-state absorption cross-section σ_{13} is evaluated by $\sigma_{13} = \alpha_0/N$, where α_0 is determined from the absorption spectrum in boric acid at 650 nm, and N (in units of no. of molecules/cm³) is the

sample concentration. The results are listed in Table 3.

For the porphyrin derivatives dissolved in solution or doped in a solid matrix, the saturable absorption has been determined at wavelengths close to the λ_{\max} of B(0,0) band, and characterized by the smaller excited-state absorption cross-section than that of the ground state [5,9]. Here we observe saturation absorption at 650 nm, which is close to the λ_{\max} of the Q(0,0) bands (see Fig. 4(b)). The result also displays that the ratio of σ_{24}/σ_{13} is less than one; this ratio is about 0.18 in average of five compounds in Table 3.

The saturation intensity can be estimated from $I_s = (h\nu)/(\tau_{21}\sigma_{24})$: for PbTMPP, we find $I_s = 3.92 \times 10^3$ W/cm² with $\tau_{21} \approx 200$ μ s obtained from the flash photolysis experiment [9]. Due to its extremely long lifetime of the lowest triplet state (≥ 100 ms), the saturation intensity for a fluorescein-doped boric acid glass is only 1.5×10^{-2} W/cm² [13]. Data in Table 3 exhibit that changing of the central metal ion has little or no effect on those parameters such as the excited-state absorption cross-section and saturation intensity.

4. Conclusions

In this study, the nonlinear response of five metal porphyrins doped in boric acid glass are measured with nanosecond laser pulses with linear polarization. The results show two-photon absorption (TPA) at near infrared, and saturation absorption (SA) at 650 nm. The values of TPA

Table 3
Saturation absorption parameters of metal TMPP doped in boric acid glass at 650 nm

Compounds	Ground state absorption cross-section σ_{13} ($\times 10^{-18}$ cm ²)	Linear absorption coefficient α_0 (cm ⁻¹)	Excited-state absorption cross-section σ_{24} ($\times 10^{-19}$ cm ²)	Saturation intensity I_s ($\times 10^3$ W/cm ²)
GaClTMPP	2.05	119.1	3.74	4.10
InClTMPP	2.12	119.1	3.83	4.02
TiClTMPP	1.93	113.9	3.63	4.21
SnTMPP	1.99	116.5	3.36	4.55
PbTMPP	2.00	120.4	3.91	3.92

The excitation pulse is linear polarized with horizontal polarization.

cross-sections δ are determined in this work, and we also propose tentatively the two-photon allowed transition states to be ${}^1B_{1g}^*$ and ${}^1B_{2g}^*$. Using both the circular and linear polarized light at 1320 nm, we obtain the polarization ratio Ω ($\Omega = \delta_{\text{circ}}/\delta_{\text{lin}}$) equals 1.40 (from InCITMPP) and 1.43 (from GaCITMPP). We are arranged to determine this ratio from some specific wavelengths (e.g. 840 and 1200 nm) to confirm these excited states. The characteristic of SA is demonstrated by the smaller excited-state absorption cross-sections than that of the ground state, and there are no significant change of the excited-state absorptivity and the saturation intensity I_s by changing of the central metal ion in this experiments.

Acknowledgements

We gratefully acknowledge the financial support from the National Science Council of ROC, Taiwan (NSC 89-2113-M-037-008). We also appreciate our referee's valuable comments to this work.

References

- [1] D.V.G.L.N. Rao, F.J. Aranda, J.F. Roach, D.E. Remy, *Appl. Phys. Lett.* 58 (1991) 1241.
- [2] G.L. Wood, M.J. Miller, A.G. Mott, *Opt. Lett.* 20 (1995) 973.
- [3] W.J. Blau, H. Byrne, W.M. Dennis, J.M. Kelly, *Opt. Commun.* 56 (1985) 25.
- [4] F.M. Qureshi, S.J. Martin, X. Long, D.D.C. Bradley, F.Z. Henari, W.J. Blau, E.C. Smith, C.H. Wang, A.K. Kar, H.L. Anderson, *Chem. Phys.* 231 (1998) 87.
- [5] F.Z. Henari, W.J. Blau, L.R. Milgram, G. Yahioglu, D. Phillips, J.A. Lacey, *Chem. Phys. Lett.* 267 (1997) 229.
- [6] S.V. Rao, N.K.M.N. Srinivas, D.N. Rao, L. Giribabu, B.G. Maiya, R. Philip, G.R. Kumar, *Opt. Commun.* 182 (2000) 255.
- [7] N. Ono, S. Ito, C.H. Wu, C.H. Chen, T.C. Wen, *Chem. Phys.* 262 (2000) 467.
- [8] P.P. Kiran, N.K.M.N. Srinivas, D.R. Reddy, B.G. Maiya, A. Dharmadhikari, A.S. Sandhu, G.R. Kumar, D.N. Rao, *Opt. Commun.* 202 (2002) 347.
- [9] K. Kandasamy, P.N. Puntambekar, B.P. Singh, S.J. Shetty, T.S. Srivastava, *J. Nonlinear Opt. Phys. Mat.* 6 (1997) 361.
- [10] K. Kandasamy, S.J. Shetty, P.N. Puntambekar, T.S. Srivastava, T. Kundu, B.P. Singh, *Chem. Commun.* (1997) 1159.
- [11] A.C. Chan, J. Dalton, L.R. Milgrom, *J. Chem. Soc. Perkin Trans. II* (1982) 707.
- [12] E.C.A. Ojadi, H. Linschitz, M. Gouterman, R.I. Walter, J.S. Lindsey, R.W. Wagner, P.R. Droupadi, W. Wang, *J. Phys. Chem.* 97 (1993) 13192.
- [13] M.A. Kramer, W.R. Tompkin, R.W. Boyd, *Phys. Rev. A* 34 (1986) 2026.
- [14] B.R. Reddy, P. Venkateswarlu, *J. Opt. Soc. Am. B* 10 (1993) 438.
- [15] W. Zhao, P. Plaffy-Muhoray, *Appl. Phys. Lett.* 63 (1993) 1613.
- [16] J.S. Shirk, R.G.S. Pong, S.R. Flom, H. Heckmann, M. Hanack, *J. Phys. Chem. A* 104 (2000) 1438.
- [17] D. Dolphin (Ed.), *The Porphyrins*, vol. III, Academic Press, New York, 1978 (Chapter 1–3).
- [18] K.K. Sundaram, *Photochemistry of Polypyridine and of Porphyrin Complexes*, Academic Press, San Diego, 1992.
- [19] E.C.A. Ojadi, H. Linschitz, M. Gouterman, R.I. Walter, J.S. Lindsey, R.W. Wagner, P.R. Droupadi, W. Wang, *J. Phys. Chem.* 97 (1993) 13192.
- [20] R.R. Birge, B.M. Pierce, *J. Chem. Phys.* 84 (1986) 3901.
- [21] R.R. Birge, B.M. Pierce, *J. Chem. Phys.* 70 (1979) 165, and the references cited therein.
- [22] G.M. Maggiora, *J. Am. Chem. Soc.* 95 (1973) 6555.
- [23] M. Sheik-Bahae, A.A. Said, T.H. Wei, D.J. Hagan, E.W. Van Stryland, *IEEE J. Quantum Electron.* 26 (1990) 760.
- [24] L.W. Tutt, T.F. Boggess, *Prog. Quantum Electron.* 17 (1993) 299.
- [25] M. Hercher, *Appl. Opt.* 6 (1967) 947.